# Heavy quark physics in the covariant quark model

*Mikhail A. Ivanov*

BLTP JINR, 141980 Dubna, Russia

I give a short introduction to the covariant quark model and its applications to heavy quark physics. The special emphasis will be devoted to the semileptonic, rare and radiative decays of the $\Lambda_b$-baryon.

## 1 Introduction

This lecture is supposed to be a mini–review of the recent results obtained by the Dubna-Mainz-Tübingen Collaboration, see Refs. [1, 2, 3]. The research is aiming to study the semileptonic, rare and radiative decays of the $\Lambda_b$-baryon by using the covariant quark model previously developed by us.

The decay $\Lambda_b \to \Lambda\,\ell^+\ell^-$ $(\ell = e, \mu, \tau)$ is a rare $b - s$ favor-changing neutral current process that in the Standard Model proceeds through electroweak loop (penguin and $W-$box) diagrams. This decay can be considered to be a welcome complement to the well–analyzed rare meson decays $B \to K^{(*)}\,\ell^+\ell^-$, $B_s \to \phi\,\ell^+\ell^-$ etc. to study the short– and long–distance dynamics of rare decays induced by the transition $b \to s\,\ell^+\ell^-$. However, the study of baryon decays is of more interest because the $\Lambda_b$ baryon has spin one half compare with zero spin of the $B-$meson. Therefore, the matrix element of the baryon decay possesses more rich helicity structure.

For the first time, the CDF Collaboration has reported on the measurement of the $\Lambda_b \to \Lambda + \mu^+\mu^-$ total branching ratio: $\mathcal{B}(\Lambda_b \to \Lambda + \mu^+\mu^-) = (1.73 \pm 0.42 \pm 0.55)\cdot 10^{-6}$ [4]. Recently, the LHCb Collaboration [5] has measured the differential branching fraction of this decay as a function of the square of the dimuon invariant mass. Integrating the differential branching fraction gives a branching fraction of $\mathcal{B}(\Lambda_b \to \Lambda+\mu^+\mu^-) = (0.96\pm0.16\pm0.13\pm0.21)\cdot10^{-6}$. Here, the uncertainties are statistical, systematic and due to the normalisation mode, $\Lambda_b \to \Lambda J/\psi$, respectively. The physics of heavy baryon decays appears to have entered a new era with these experimental results.

There have been a number of theoretical papers on the rare $\Lambda_b \to \Lambda$ baryon decays involving the one-photon mode $\Lambda_b \to \Lambda\gamma$ and the dilepton modes $\Lambda_b \to \Lambda\,\ell^+\ell^-$ $(\ell = e, \mu, \tau)$. They use the same set of (penguin) operators or their non–Standard Model extensions to describe the short distance dynamics but differ in their use of theoretical models to calculate the nonperturbative transition matrix element $\langle\Lambda|\,O_i\,|\Lambda_b\rangle$.

We use the covariant constituent quark model (for short: covariant quark model) as dynamical input to calculate the nonperturbative transition matrix elements. In the covariant quark model the current–induced transitions between baryons are calculated from two–loop Feynman diagrams with free quark propagators in which the divergent high energy behavior of the loop integrations is tempered by Gaussian vertex functions. Quark confinement has incorporated in an effective way, first, by introducing the scale integration in the space of $\alpha$-parameters, and, second, by cutting this scale integration on the upper limit which corresponds to an infrared

cutoff. In this manner one removes all possible thresholds presented in the initial quark diagram. The cutoff parameter is taken to be the same for all physical processes. We adjust other model parameters by fitting the calculated quantities of the basic physical processes to available experimental data. One has to emphasize that the covariant quark model is a truly frame–independent field–theoretic quark model in contrast to other constituent quark models which are basically quantum mechanical with built–in relativistic elements. One of the advantages of the covariant quark model is that it allows one to calculate the transition form factors in the full accessible range of $q^2$–values.

We review the basic notions of our dynamical approach — *the covariant quark model for baryons*. In particular, we derive the phenomenological Lagrangians describing the interaction of baryons with their constituent quarks. Then we introduce the corresponding interpolating 3–quark currents with the quantum numbers of the respective baryon and discuss the idea and implementation of quark confinement. Finally, we apply our approach to the rare one-photon decay $\Lambda_b \to \Lambda\gamma$ and the dilepton decay $\Lambda_b \to \Lambda(\to p\pi^-) + j_{\rm eff}(\to \ell^+\ell^-)$. We present a detailed discussion of the helicity formalism that allows one to write down the joint angular distribution of the cascade decay $\Lambda_b \to \Lambda(\to p\pi^-) + j_{\rm eff}(\to \ell^+\ell^-)$.

## 2 The covariant quark model for baryons

In the following we consider $\Lambda = (Q[ud])$-type baryons needed in the present application. They consist of a heavy quark and two light quarks in a ${}^1S_0$ spin 0 configuration. The coupling of a $\Lambda$-type baryon to its constituent quarks is described by the Lagrangian

$$\begin{aligned}
\mathcal{L}^{\Lambda}_{\rm int}(x) &= g_\Lambda\, \bar\Lambda(x)\cdot J_\Lambda(x) + g_\Lambda\, \bar J_\Lambda(x)\cdot\Lambda(x)\,,\\
J_\Lambda(x) &= \int dx_1\int dx_2\int dx_3\, F_\Lambda(x;x_1,x_2,x_3)\, J^{(\Lambda)}_{3q}(x_1,x_2,x_3)\,,\\
J^{(\Lambda)}_{3q}(x_1,x_2,x_3) &= \epsilon^{a_1a_2a_3}\, Q^{a_1}(x_1)\, u^{T\,a_2}(x_2)\, C\,\gamma^5\, d^{a_3}(x_3)\,,\\
\bar J_\Lambda(x) &= J^\dagger_\Lambda(x)\gamma^0\,,
\end{aligned}$$

where $Q = s, c, b$. Here the matrix $C = \gamma^0\gamma^2$ is the usual charge conjugation matrix and the $a_i$ $(i = 1, 2, 3)$ are color indices.

The vertex function $F_\Lambda$ characterizes the finite size of the $\Lambda$-type baryon. We assume that the vertex function is real. To satisfy translational invariance the function $F_N$ has to fulfill the identity

$$F_\Lambda(x+a;x_1+a,x_2+a,x_3+a) \,=\, F_\Lambda(x;x_1,x_2,x_3)$$

for any given four-vector $a$. In the following we use a particular form for the vertex function

$$F_\Lambda(x;x_1,x_2,x_3) \,=\, \delta^{(4)}(x - \sum_{i=1}^{3} w_i x_i)\; \Phi_\Lambda\Big(\sum_{i<j}(x_i-x_j)^2\Big) \qquad (1)$$

where $\Phi_\Lambda$ is the correlation function of the three constituent quarks with the coordinates $x_1$, $x_2$, $x_3$ and masses $m_1$, $m_2$, $m_3$, respectively. The variable $w_i$ is defined by $w_i = m_i/(m_1+m_2+m_3)$ such that $\sum_{i=1}^3 w_i = 1$.

We shall make use of the Jacobi coordinates $\rho_{1,2}$ and the CM coordinate $x$ which are defined by

$$\begin{aligned} x_1 &= x + \tfrac{1}{\sqrt{2}}\, w_3\, \rho_1 - \tfrac{1}{\sqrt{6}}\, (2w_2 + w_3)\, \rho_2\,, \\ x_2 &= x + \tfrac{1}{\sqrt{2}}\, w_3\, \rho_1 + \tfrac{1}{\sqrt{6}}\, (2w_1 + w_3)\, \rho_2\,, \\ x_3 &= x - \tfrac{1}{\sqrt{2}}\, (w_1 + w_2)\, \rho_1 + \tfrac{1}{\sqrt{6}}\, (w_1 - w_2)\, \rho_2\,. \end{aligned}$$

The CM coordinate is given by $x = \sum_{i=1}^{3} w_i x_i$. In terms of the Jacobi coordinates one obtains

$$\sum_{i<j} (x_i - x_j)^2 = \rho_1^2 + \rho_2^2\,.$$

Note that the choice of Jacobi coordinates is not unique. By using the particular choice of Jacobi coordinates given by Eq. (2) one obtains the following representation for the correlation function $\Phi_\Lambda$ in Eq. (1)

$$\begin{aligned} \Phi_\Lambda\Big(\sum_{i<j}(x_i - x_j)^2\Big) &= \int \frac{d^4p_1}{(2\pi)^4} \int \frac{d^4p_2}{(2\pi)^4}\, e^{-ip_1(x_1-x_3)-ip_2(x_2-x_3)}\, \bar{\Phi}_\Lambda(-P_1^2 - P_2^2)\,, \qquad (2) \\ \bar{\Phi}_\Lambda(-P_1^2 - P_2^2) &= \tfrac{1}{9} \int d^4\rho_1 \int d^4\rho_2\, e^{iP_1\rho_1 + iP_2\rho_2}\, \Phi_\Lambda(\rho_1^2 + \rho_2^2)\,, \\ & \quad P_1 = \tfrac{1}{\sqrt{2}}(p_1 + p_2)\,, \qquad P_2 = -\tfrac{1}{\sqrt{6}}(p_1 - p_2)\,. \end{aligned}$$

This representation is valid for any choice of the set of Jacobi coordinates. The particular choice (2) is a preferred choice since it leads to the specific form of the argument $-P_1^2 - P_2^2 = -\frac{2}{3}(p_1^2 + p_2^2 + p_1 p_2)$. Since this expression is invariant under the transformations: $p_1 \leftrightarrow p_2$, $p_2 \to -p_2 - p_1$ and $p_1 \to -p_1 - p_2$, the r.h.s. in Eq. (2) is invariant under permutations of all $x_i$ as it should be.

In the next step we have to specify the function $\bar{\Phi}_\Lambda(-P_1^2 - P_2^2) \equiv \bar{\Phi}_\Lambda(-P^2)$ which characterizes the finite size of the baryons. We will choose a simple Gaussian form for the function $\bar{\Phi}_\Lambda$:

$$\bar{\Phi}_\Lambda(-P^2) = \exp(P^{\,2}/\Lambda_\Lambda^2)\,, \qquad (3)$$

where $\Lambda_\Lambda$ is a size parameter parametrized the distribution of quarks inside a $\Lambda$-type baryon. We use different values of the $\Lambda_\Lambda$ parameter for different types of the $\Lambda$-type baryon: $\Lambda_{\Lambda_s}$, $\Lambda_{\Lambda_c}$ and $\Lambda_{\Lambda_b}$ for the $\Lambda$, $\Lambda_c$ and $\Lambda_b$ baryons, respectively.

Since $P^{\,2}$ turns into $-P_E^2$ in Euclidean space the form (3) has the appropriate falloff behavior in the Euclidean region. We emphasize that any choice for $\Phi_\Lambda$ is appropriate as long as it falls off sufficiently fast in the ultraviolet region of Euclidean space to render the corresponding Feynman diagrams ultraviolet finite. The choice of a Gaussian form for $\Phi_\Lambda$ has obvious calculational advantages.

The coupling constants $g_\Lambda$ are determined by the compositeness condition suggested by Weinberg [6] and Salam [7] (for review, see Ref. [8]) and extensively used in our approach (for details, see Ref. [9]). The compositeness condition in the case of baryons implies that the renormalization constant of the baryon wave function is set equal to zero:

$$Z_\Lambda = 1 - \Sigma'_\Lambda(m_\Lambda) = 0$$

where $\Sigma'_\Lambda$ is the on-shell derivative of the $\Lambda$-type baryon mass function $\Sigma_\Lambda$, i.e. $\Sigma'_\Lambda = \partial\,\Sigma_\Lambda/\partial\not{p}$, at $\not{p} = m_\Lambda$. The compositeness condition is the central equation of our covariant quark model. The physical meaning, the implications and corollaries of the compositeness condition have been discussed in some detail in our previous papers (see e.g. [10]).

## 2.1 Infrared confinement

We have shown in [10] how the confinement of quarks can be effectively incorporated in the covariant quark model. In a first step, we introduced an additional scale integration in the space of Schwinger's $\alpha$–parameters with an integration range from zero to infinity. In a second step the scale integration was cut off at the upper limit which corresponds to the introduction of an infrared (IR) cutoff. In this manner all possible thresholds present in the initial quark diagram were removed. The cutoff parameter was taken to be the same for all physical processes. Other model parameters such as the constituent quark masses and size parameters were determined from a fit to experimental data.

Let us describe the basic features of how IR confinement is implemented in our model. All physical matrix elements are described by Feynman diagrams written in terms of a convolution of free quark propagators and the vertex functions. In computation of Feynman diagrams we use, in the momentum space, the Schwinger representation of the quark propagator

$$S(k) = \frac{m + \not{k}}{m^2 - k^2} = (m + \not{k}) \int\limits_0^\infty d\alpha\, e^{-\alpha\left(m^2 - k^2\right)}\,.$$

The general form of a resulting Feynman diagrams is

$$\Pi\left(p_1, \ldots, p_m\right) = \int\limits_0^\infty d^n\alpha \int \left[d^4k\right]^\ell \Phi \times \exp\left\{-\sum_{i=1}^n \alpha_i \left[m_i^2 - \left(K_i + P_i\right)^2\right]\right\}, \qquad (4)$$

where $K_i$ represents a linear combination of loop momenta, $P_i$ stands for a linear combination of external momenta and $\Phi$ refers to the numerator product of propagators and vertex functions. The integrand in Eq. (4) has a Gaussian form with the exponential factor

$$kak + 2kr + R = k_i a_{ij} k_j + 2k_i r_i + R, \qquad (i, j = 1, \ldots, \ell),$$

where $k_i$ is a 4-vector of the "i"-loop integration, $a$ is a $\ell \times \ell$ matrix depending on the parameters $\alpha_i$ and size parameters $\Lambda$, $r_i$ is a 4- vector composed from the external momenta $p_i$ and $R$ is a quadratic form of the external momenta. Tensor loop integrals are calculated with the help of the differential representation

$$k_i^\mu e^{2kr} = \frac{1}{2}\frac{\partial}{\partial r_{i\,\mu}} e^{2kr}\,,$$

which in general may be written in the form

$$\int \left[d^4k\right]^\ell P\left(k\right) e^{kak + 2kr + R} = \int \left[d^4k\right]^\ell P\left(\frac{1}{2}\frac{\partial}{\partial r}\right) e^{kak + 2kr + R} = P\left(\frac{1}{2}\frac{\partial}{\partial r}\right) \int \left[d^4k\right]^\ell e^{kak + 2kr + R},$$

where the polynomial operator means $P(k) = k_1^{\mu_1} \ldots k_m^{\mu_m}$. After doing the loop integration the differential operators $\partial/\partial r_{i\,\mu}$ will give cause to outer momenta tensors. It may be done in

effective way by using the identity

$$\int\limits_0^\infty d^n\alpha\, P\left(\frac{1}{2}\frac{\partial}{\partial r}\right) e^{-\frac{r^2}{a}} = \int\limits_0^\infty d^n\alpha\, e^{-\frac{r^2}{a}}\, P\left(\frac{1}{2}\frac{\partial}{\partial r} - \frac{r}{a}\right).$$

The calculation of the polynomial $P\left(\frac{1}{2}\frac{\partial}{\partial r} - \frac{r}{a}\right)$ can be automized by using the commutator $[\frac{\partial}{\partial r_i^\mu}, r_j^\nu] = \delta_{ij}\, g^{\mu\nu}$. We have written a FORM [11] program that achieves the necessary commutations of the differential operators in a very efficient way.

The last point which remains to be discussed is the infrared cut-off we impose on the integration over the Schwinger parameters. This integration is multidimensional with the limits from 0 to $+\infty$. In order to arrive to a single cut-off parameter we firstly transform the integral over an infinite space into an integral over a simplex convoluted with only one-dimensional improper integral. For that purpose we use the $\delta$-function form of the identity

$$1 = \int\limits_0^\infty \mathrm{dt}\, \delta\left(\mathrm{t} - \sum_{\mathrm{i}=1}^{\mathrm{n}} \alpha_{\mathrm{i}}\right), \qquad (\forall \alpha_{\mathrm{i}} \geq 0)$$

from which follows

$$\Pi = \int\limits_0^\infty dt\, t^{n-1} \int\limits_0^1 d^n\alpha\, \delta\left(1 - \sum_{i=1}^{n} \alpha_i\right) \times W\left(t\alpha_1, \ldots, t\alpha_1\right),$$

where $W$ represents the integrand of Schwinger parameters. The cut-off $\lambda$ is then introduced in a natural way

$$\int\limits_0^\infty dt\, t^{n-1} \ldots \to \int\limits_0^{1/\lambda^2} dt\, t^{n-1} \ldots.$$

Such a cut-off makes the integral to be an analytic function without any singularities. In this way all potential thresholds in the quark loop diagrams are removed together with corresponding branch points [10]. Within covariant quark model the cut-off parameter is universal for all processes and its value, as obtained from a fit to data, is

$$\lambda_{\mathrm{cut-off}} = 0.181\ \mathrm{GeV}.$$

The numerical evaluations have been done by a numerical program written in the FORTRAN code.

## 3 The rare baryon decays $\Lambda_b \to \Lambda + \ell^+\ell^-$ and $\Lambda_b \to \Lambda + \gamma$

The effective Hamiltonian [12] leads to the quark decay amplitudes $b \to s l^+ l^-$ and $b \to s\gamma$:

$$\begin{aligned} M(b \to s\ell^+\ell^-) &= \frac{G_F}{\sqrt{2}}\frac{\alpha\lambda_t}{2\pi}\left\{C_9^{\mathrm{eff}}\ (\bar{s}O^\mu b)\ \left(\bar{\ell}\gamma_\mu\ell\right) + C_{10}\,(\bar{s}O^\mu b)\ \left(\bar{\ell}\gamma_\mu\gamma_5\ell\right)\right. \\ &- \left.\frac{2}{q^2}\,C_7^{\mathrm{eff}}\ \left[m_b\left(\bar{s}\, i\sigma^{\mu q}\left(1+\gamma^5\right)\, b\right) + m_s\left(\bar{s}\, i\sigma^{\mu q}\left(1-\gamma^5\right)\, b\right)\right]\left(\bar{\ell}\gamma_\mu\ell\right)\right\} \end{aligned}$$

and

$$M(b\to s\gamma) \;=\; -\frac{G_F}{\sqrt{2}}\frac{e\lambda_t}{4\pi^2}\,C_7^{\rm eff}\,\Big[m_b\left(\bar s\, i\sigma^{\mu q}\,(1+\gamma^5)\;b\right)+m_s\left(\bar s\, i\sigma^{\mu q}\,(1-\gamma^5)\;b\right)\Big]\,\epsilon_\mu\,,$$

where $\sigma^{\mu q}=\frac{i}{2}(\gamma^\mu\gamma^\nu-\gamma^\nu\gamma^\mu)q_\nu$, $O^\mu=\gamma^\mu(1-\gamma^5)$ and $\lambda_t\equiv V_{ts}^\dagger V_{tb}$.

The Wilson coefficient $C_9^{\rm eff}$ effectively takes into account, first, the contributions from the four-quark operators $Q_i(i=1,\cdots,6)$ and, second, the nonperturbative effects (long–distance contributions) coming from the $c\bar c$-resonance contributions what are, as usual, parametrized by a Breit-Wigner ansatz [13].

The Feynman diagrams contributing to the exclusive transitions $\Lambda_b\to\Lambda\bar\ell\ell$ and $\Lambda_b\to\Lambda\gamma$ are shown in Fig. 1.

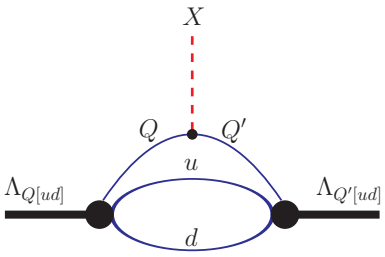


Figure 1: Diagrams contributing to the flavor-changing transition $\Lambda_{Q[ud]}\to\Lambda_{Q'[ud]}+X$ , where $X=\ell^-\bar\nu_\ell,\ell^+\ell^-$ or $\gamma$.

The corresponding matrix elements of the exclusive transitions $\Lambda_b\to\Lambda\bar\ell\ell$ and $\Lambda_b\to\Lambda\gamma$ are defined by

$$\begin{aligned}
M(\Lambda_b\to\Lambda\bar\ell\ell) \;&=\; \frac{G_F}{\sqrt{2}}\frac{\alpha\lambda_t}{2\,\pi}\Big\{C_9^{\rm eff}\,\langle\Lambda\,|\,\bar s\,O^\mu\,b\,|\,\Lambda_b\rangle\,\bar\ell\gamma_\mu\ell\\
&+\; C_{10}\,\langle\Lambda\,|\,\bar s\,O^\mu\,b\,|\,\Lambda_b\rangle\,\bar\ell\gamma_\mu\gamma_5\ell\\
&-\; \frac{2m_b}{q^2}\,C_7^{\rm eff}\,\langle\Lambda\,|\,\bar s\,i\sigma^{\mu q}\,(1+\gamma^5)\;b\,|\,\Lambda_b\rangle\,\bar\ell\gamma_\mu\ell\Big\}
\end{aligned}\tag{5}$$

and

$$M(\Lambda_b\to\Lambda\gamma)=-\frac{G_F}{\sqrt{2}}\frac{e\lambda_t}{4\,\pi^2}\,m_b\,C_7^{\rm eff}\,\langle\Lambda\,|\,\bar s\,i\sigma^{\mu q}\,(1+\gamma^5)\;b\,|\,\Lambda_b\rangle\,\epsilon_\mu\,.\tag{6}$$

The hadronic matrix elements in Eqs. (5) and (6) are expanded in terms of dimensionless form factors $f_i^J$ $(i=1,2,3$ and $J=V,A,TV,TA)$, viz.

$$\begin{aligned}
\langle B_2\,|\,\bar s\,\gamma^\mu\,b\,|B_1\rangle \;&=\; \bar u_2(p_2)\Big[f_1^V(q^2)\gamma^\mu-f_2^V(q^2)i\sigma^{\mu q}/M_1+f_3^V(q^2)q^\mu/M_1\Big]u_1(p_1)\,,\\
\langle B_2\,|\,\bar s\,\gamma^\mu\gamma^5\,b\,|B_1\rangle \;&=\; \bar u_2(p_2)\Big[f_1^A(q^2)\gamma^\mu-f_2^A(q^2)i\sigma^{\mu q}/M_1+f_3^A(q^2)q^\mu/M_1\Big]\gamma^5u_1(p_1)\,,\\
\langle B_2\,|\,\bar s\,i\sigma^{\mu q}/M_1\,b\,|B_1\rangle \;&=\; \bar u_2(p_2)\Big[f_1^{TV}(q^2)(\gamma^\mu q^2-q^\mu\,\not q)/M_1^2-f_2^{TV}(q^2)i\sigma^{\mu q}/M_1\Big]u_1(p_1)\,,\\
\langle B_2\,|\,\bar s\,i\sigma^{\mu q}\gamma^5/M_1\,b\,|B_1\rangle \;&=\; \bar u_2(p_2)\Big[f_1^{TA}(q^2)(\gamma^\mu q^2-q^\mu\,\not q)/M_1^2-f_2^{TA}(q^2)i\sigma^{\mu q}/M_1\Big]\gamma^5u_1(p_1)\,.
\end{aligned}$$

Here, $p_1,M_1$ and $p_2,M_2$ are momenta and masses of the ingoing and outgoing baryons, respectively. The transfer momentum is equal to $q=p_1-p_2$. One can see that, in comparison with the Cabibbo-allowed $b\to c$ and $c\to s$ transitions, one has four more form factors $f_{1,2}^{TV,TA}$.

The $\Lambda_b\to\Lambda\gamma$ decay rate is calculated according to

$$\Gamma(\Lambda_b\to\Lambda\gamma)=\frac{\alpha}{2}\left(\frac{G_F m_b\,|\lambda_t|\,C_7^{\rm eff}}{4\pi^2\sqrt{2}}\right)^2\frac{(M_1^2-M_2^2)^3}{M_1^3}\;\left[\Big(f_2^{TV}(0)\Big)^2\;+\Big(f_2^{TA}(0)\Big)^2\right].$$

The angular decay distribution for the cascade decay $\Lambda_b \to \Lambda(\to p\pi^-)\gamma$ can be written as

$$\frac{1}{\Gamma_{\rm tot}}\frac{d\Gamma(\Lambda_b \to \Lambda(\to p\pi^-)\gamma)}{d\cos\theta_B} = {\rm Br}(\Lambda \to p\pi^-)\,\frac{1}{2}\,{\rm Br}(\Lambda_b \to \Lambda\gamma)(1-\alpha_B\cos\theta_B)\,,$$

where $\alpha_B$ is the asymmetry parameter in the decay $\Lambda \to p + \pi^-$ for which we take the experimental value $\alpha_B = 0.642 \pm 0.013$ [14].

As in the case of the rare meson decays $B \to K^{(*)}\ell^+\ell^-$ ($\ell = e, \mu, \tau$) treated in [15] one can exploit the cascade nature of the decay $\Lambda_b \to \Lambda(\to p\pi^-) + j_{\rm eff}(\to \ell^+\ell^-)$ to write down a joint angular decay distribution involving the polar angles $\theta$, $\theta_B$ and the azimuthal angles $\chi$ defined by the decay products in their respective (center of mass) CM systems as shown in Fig. 2.

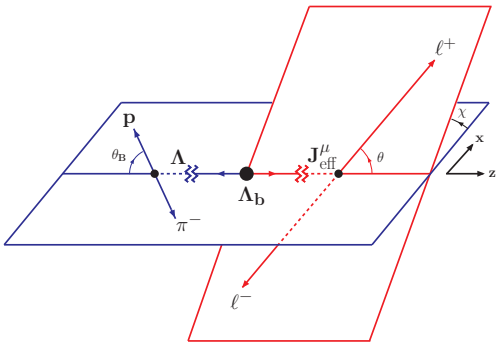


Figure 2: Definition of angles $\theta$, $\theta_B$ and $\chi$ in the cascade decay $\Lambda_b \to \Lambda(\to p\pi^-) + J_{\rm eff}(\to \ell^+\ell^-)$.

We write out the three-fold angular decay distribution in a manner where we collect together terms with the threshold behavior in a factor $v = \sqrt{1-4m_\ell^2/q^2}$ : $v^0$, $v^1$ and $v^2$. Including the $q^2$ dependence one obtains a four-fold joint angular decay distribution for the decay of an unpolarized $\Lambda_b$. One has

$$W(\theta,\theta_B,\chi) \propto \frac{32\,q^2}{9}\left(A\,v^2 + B\,v + C\,\frac{2m_\ell^2}{q^2}\right),$$

where the coefficients $A$,$B$ and $C$ are given by

$$\begin{aligned}
A &= \frac{9}{64}(1+\cos^2\theta)\,\left(U^{11}+U^{22}\right) + \frac{9}{32}\,\sin^2\theta\,\left(L^{11}+L^{22}\right)\\
&+ \frac{9}{32}\,\alpha_B\,\cos\theta_B\left[\sin^2\theta\,\left(L_P^{11}+L_P^{22}\right) + \frac{1}{2}(1+\cos^2\theta)\,\left(P^{11}+P^{22}\right)\right]\\
&+ \frac{9}{16\sqrt{2}}\,\alpha_B\,\sin 2\theta\,\sin\theta_B\left[\cos\chi\,\left(I1_P^{11}+I1_P^{22}\right) - \sin\chi\,\left(I2_P^{11}+I2_P^{22}\right)\right],\\
B &= -\frac{9}{16}\,\cos\theta\left[P^{12} + \alpha_B\,\cos\theta_B\,U^{12}\right]\\
&- \frac{9}{4\sqrt{2}}\,\alpha_B\,\sin\theta\,\sin\theta_B\left[\cos\chi\,I3_P^{12} - \sin\chi\,I4_P^{12}\right],\\
C &= \frac{9}{16}\,\left(U^{11}+L^{11}+S^{22}\right) + \frac{9}{16}\,\alpha_B\,\cos\theta_B\,\left(P^{11}+L_P^{11}+S_P^{22}\right).
\end{aligned}$$

We have adopted the notations

$$X^{mm'} \equiv \frac{d\Gamma_X^{mm'}}{dq^2} = \frac{1}{2}\frac{G_F^2}{(2\pi)^3}\left(\frac{\alpha|\lambda_t|}{2\pi}\right)^2\frac{|\mathbf{p_2}|\,q^2\,v}{12\,M_1^2}\,H_X^{mm'}\,,$$

where the bilinear expressions $H_X^{mm'}$ $(X = U, L, S, P, L_P, S_P, I1_P, I2_P, I3_P, I4_P)$ are defined in Ref. [2]. Here, $|\mathbf{p_2}| = \lambda^{1/2}(M_1^2, M_2^2, q^2)/2M_1$ is the momentum of the $\Lambda$-hyperon in the $\Lambda_b$-rest frame. Note that we have included the statistical factor $1/(2S_{\Lambda_b}+1) = 1/2$ in the definition of the rate functions.

Putting in the correct normalization factors one obtains the differential rate $d\Gamma/dq^2$ which reads

$$\frac{d\Gamma(\Lambda_b \to \Lambda\, \ell^+\ell^-)}{dq^2} = \frac{v^2}{2}\cdot\left(U^{11+22} + L^{11+22}\right) + \frac{2m_\ell^2}{q^2}\cdot\frac{3}{2}\cdot\left(U^{11} + L^{11} + S^{22}\right),$$

Here, and in the following, we do an importance sampling of our rate expressions by sorting the contributions according to powers of the threshold factor $v$. When one wants to compare our results to the corresponding results for the mesonic case written down in Ref. [15] one has to rearrange the contributions in Ref. [15] accordingly. And, one has to take into account the factor of 3 difference in the definition of the scalar structure function.

The total rate, finally, is obtained by $q^2$–integration in the range

$$4m_\ell^2 \;\le\; q^2 \;\le\; (M_1 - M_2)^2\,.$$

For the lower $q^2$ limit one has $4m_\ell^2 = (1.04\times 10^{-6}, 0.045, 12.6284)$ GeV$^2$ for $\ell = (e, \mu, \tau)$. The upper limit of the $q^2$–integration is given by $(M_{\Lambda_b} - M_\Lambda)^2 = 20.29$ GeV$^2$. For $\ell = (e, \mu)$ one is practically probing the whole $q^2$ region while for $\ell = \tau$ the $q^2$–range is restricted to the low recoil half of phase-space starting at $\sqrt{q^2} = 3.55$ GeV just below the position of the $\Psi(2S)$ vector meson resonance.

# 4 Numerical results

With the choice of dimensional parameters $\Lambda_{\Lambda_s} = 0.490$ GeV, $\Lambda_{\Lambda_c} = 0.864$ GeV and $\Lambda_{\Lambda_b} = 0.569$ GeV we get a reasonable agreement with current data on exclusive Cabibbo-allowed decays of $\Lambda_c$ and $\Lambda_b$ as one can see from the Table 1.

| Mode | Our results | Data [14] |
|---|---|---|
| $\Lambda_c \to \Lambda e^+\nu_e$ | 2.0 | $2.1 \pm 0.6$ |
| $\Lambda_c \to \Lambda \mu^+\nu_\mu$ | 2.0 | $2.0 \pm 0.7$ |
| $\Lambda_b \to \Lambda_c e^-\bar\nu_e$ | 6.6 | $6.5^{+3.2}_{-2.5}$ |
| $\Lambda_b \to \Lambda_c \mu^-\bar\nu_\mu$ | 6.6 | |
| $\Lambda_b \to \Lambda_c \tau^-\bar\nu_\tau$ | 1.8 | |

Table 1: Branching ratios of semileptonic decays of heavy baryons (in %).

For the magnetic moments we get the following results:

$$\mu_{\Lambda_s} = -0.73\,, \quad \mu_{\Lambda_c} = 0.39\,, \quad \mu_{\Lambda_b} = -0.06\,,$$

which compares well with data for the $\mu_{\Lambda_s}$ and theoretical estimates for the $\mu_{\Lambda_c}$ and $\mu_{\Lambda_b}$ (see the detailed discussion in Ref. [16]).

In particular, our present results for the magnetic moments of heavy $\Lambda$-hyperons are very close to our predictions done before in the model without taking account of the mechanism of quark confinement: $\mu_{\Lambda_c} = 0.42$ and $\mu_{\Lambda_b} = -0.06$ [16].

We present our results for the branching ratios of the rare dileptonic decay $\Lambda_b \to \Lambda\ell^+\ell^-$ in Table 2. The results without long-distance effects are shown in brackets. Our predictions for the radiative decay $\Lambda_b \to \Lambda\gamma$ are also displayed.

In our calculations we do not include the regions around the two charmonium resonances $R_{c\bar c} = J/\psi, \Psi(2S)$. We exclude the regions $M_{J/\Psi} - 0.20$ GeV to $M_{J/\Psi} + 0.04$ GeV and $M_{\Psi(2S)} -$

0.10 GeV to $M_{\Psi(2S)}+0.02$ GeV. As stressed in Ref. [17] these regions are experimentally vetoed, because the rates of nonleptonic decays $\Lambda_b \to \Lambda + R_{c\bar{c}}$, followed by the dileptonic decays of the charmonium, are much larger than rates of the $b \to s$-induced rare decays $\Lambda_b \to \Lambda\ell^+\ell^-$. Vetoing the regions near the charmonium resonances leads to physically acceptable results — the predictions with and without the inclusion of long–distance effects are comparable with each other. Otherwise (without such a vetoing) the results with long–distance effects are dramatically enhanced as shown in different theoretical calculations.

| Mode | Our results | Data |
|---|---|---|
| $\Lambda_b \to \Lambda e^+e^-$ | 1.0 (1.0) | |
| $\Lambda_b \to \Lambda\mu^+\mu^-$ | 1.0 (1.0) | $0.96 \pm 0.16 \pm 0.13 \pm 0.21$ [5]<br>$1.73 \pm 0.42 \pm 0.55$ [4] |
| $\Lambda_b \to \Lambda\tau^+\tau^-$ | 0.2 (0.3) | |
| $\Lambda_b \to \Lambda\gamma$ | 4.0 | $< 1.3\,10^3$ |

Table 2: Branching ratios of rare decays $\Lambda_b \to \Lambda\ell^+\ell^-$ with (without) long–distance contributions and radiative decay $\Lambda_b \to \Lambda\gamma$ (in units of $10^{-6}$).

# 5 Summary and conclusions

We have given a short review of the covariant quark model with infrared confinement and applied this approach to describe the semileptonic, rare and radiative decays of heavy $\Lambda_b$-baryon.

We have described from a unified point of view exclusive Cabibbo-allowed semileptonic decays $\Lambda_b \to \Lambda_c\ell^-\bar{\nu}_\ell$, $\Lambda_c \to \Lambda\ell^+\nu_\ell$ and rare decays $\Lambda_b \to \Lambda\ell^+\ell^-$, $\Lambda_b \to \Lambda\gamma$ with the use of only three model parameters: the size parameters $\Lambda_{\Lambda_s}$, $\Lambda_{\Lambda_c}$ and $\Lambda_{\Lambda_b}$ defining the distribution of quarks in the $\Lambda$, $\Lambda_c$ and $\Lambda_b$ baryons.

We have used the helicity formalism to express a number of observables in the rare baryon decay $\Lambda_b \to \Lambda(\to p\pi^-)\,\ell^+\ell^-$ in terms of a basic set of hadronic helicity structure functions. In the helicity method one provides complete information on the spin density matrix of each particle in the cascade decay chain which can be conveniently read out by considering angular decay distributions in the rest frame of that particular particle. The advantage of the helicity method is that it is straightforward to define any of the observables of the problem and to express them in terms of bilinear forms of the hadronic helicity matrix elements.

The helicity formulas can be used as input in a MC event generator patterned after the existing event generator for $\Xi^0(\uparrow) \to \Sigma^+(\to p\pi^0)\ell^-\bar{\nu}_\ell$ $\ell = (e, \mu)$ which is described and put to use in [18] and which has been used by the NA48 Collaboration to analyze its data on the above decay [19].

# Acknowledgments

I am grateful to my collaborators Thomas Gutsche, Jürgen G. Körner, Valery E. Lyubovitskij and Pietro Santorelli for helpful discussions. This work was supported in part by the Heisenberg-Landau Grant and Mainz Institute for Theoretical Physics (MITP).

## References


[1] T. Gutsche, M. A. Ivanov, J. G. Körner, V. E. Lyubovitskij and P. Santorelli, Phys. Rev. **D88** 114018 (2013).

[2] T. Gutsche, M. A. Ivanov, J. G. Körner, V. E. Lyubovitskij and P. Santorelli, Phys. Rev. **D87** 074031 (2013).

[3] T. Gutsche, M. A. Ivanov, J. G. Körner, V. E. Lyubovitskij and P. Santorelli, Phys. Rev. **D86** 074013 (2012).

[4] T. Aaltonen *et al.* [ CDF Collaboration ], Phys. Rev. Lett. **107** 201802 (2011).

[5] RAaij *et al.* [LHCb Collaboration], Phys. Lett. B **B725** 25 (2013).

[6] S. Weinberg, Phys. Rev. **130** 776 (1963).

[7] A. Salam, Nuovo Cim. **25** 224 (1962).

[8] K. Hayashi, M. Hirayama, T. Muta, N. Seto and T. Shirafuji, Fortsch. Phys. **15** 625 (1967).

[9] G. V. Efimov and M. A. Ivanov, *The Quark Confinement Model of Hadrons*, (IOP Publishing, Bristol & Philadelphia, 1993).

[10] T. Branz, A. Faessler, T. Gutsche, M. A. Ivanov, J. G. Körner and V. E. Lyubovitskij, Phys. Rev. **D81** 034010 (2010).

[11] J. A. M. Vermaseren, Nucl. Phys. Proc. Suppl. **183** 19 (2008).

[12] G. Buchalla, A. J. Buras and M. E. Lautenbacher, Rev. Mod. Phys. **68** 1125 (1996).

[13] A. Ali, T. Mannel and T. Morozumi, Phys. Lett. **B273** 505 (1991).

[14] J. Beringer *et al.* [Particle Data Group Collaboration], Phys. Rev. **D86** 010001 (2012).

[15] A. Faessler, T. Gutsche, M. A. Ivanov, J. G. Körner, V. E. Lyubovitskij, Eur. Phys. J. direct **C4** 18 (2002).

[16] A. Faessler, T. .Gutsche, M. A. Ivanov, J. G. Körner, V. E. Lyubovitskij, D. Nicmorus and K. Pumsa-ard, Phys. Rev. D **D73** 094013 (2006).

[17] L. Mott and W. Roberts, Int. J. Mod. Phys. **A27** 1250016 (2012).

[18] A. Kadeer, J. G. Körner, U. Moosbrugger, Eur. Phys. J. **C59** 27 (2009).

[19] J. R. Batley *et al.* [NA48/1 Collaboration], Phys. Lett. **B720** 105 (2013).